Open Archive Toulouse Archive Ouverte (OATAO)

OATAO is an open access repository that collects the work of Toulouse researchers and makes it freely available over the web where possible.

Predicting the dynamic behaviour of torus milling tools when climb milling using the stability lobes theory

M. Mousseigne [a], Y. Landon [a,*], S. Seguy [b], G. Dessein [c], J.M. Redonnet [a]

[a] Université de Toulouse; INSA, UPS, Mines Albi, ISAE; ICA (Institut Clément Ader); Bât 3R1, 118 route de Narbonne, F-31062 Toulouse cedex 9, France
[b] Université de Toulouse; INSA, UPS, Mines Albi, ISAE; ICA (Institut Clément Ader); 135 avenue de Rangueil, F-31077 Toulouse cedex 4, France
[c] Université de Toulouse; École Nationale d'Ingénieurs de Tarbes; Laboratoire Génie de Production, 47 avenue d'Azereix, BP 1629, F-65016 Tarbes Cedex, France

A B S T R A C T

This paper investigates stability and dynamic behaviour of torus tool in climb milling on 5 positioned axes. The stability lobes theory is used to enable stable cutting conditions to be chosen. As the adaptation of such a theory to complex milling configurations is a difficult matter, new methods are presented to identify the dynamic parameters. Tool dynamic characteristics (stiffness and natural pulsation) are determined with an original coupled calculations-tests method. Start and exit angles are computed exactly using an original numerical model. A sensitivity analysis highlights the influence of machining parameters on stability of climb milling. This shows that a third region of "potential instability" must be taken into account in plotting stability lobes, due to the uncertainty of prediction due to modelling and identification of parameters. The results were validated experimentally with an innovative approach, especially through the use of high-speed cameras. Analysis of vibrations and the surface roughness allowed the analytical model to be verified so as to optimise the inclination of the tool on the surface.

1. Introduction

Climb milling (or milling with a positive lead angle) is an end milling configuration frequently encountered by mould makers and other manufacturers of complex shaped parts (for example in the medical, dental, automobile and aeronautical sectors). It is associated with the use of hemispheric or more generally torus tools, with a low diameter/length ratio, well suited to the milling of free-form surfaces. However, the local machining configuration (climb milling, milling down the slope, with lead angle) has a determinant influence on the surface quality [1]. It is advantageous to climb mill to increase the effective cutting speed on such tools and approach the programmed nominal cutting speed. But this also leads to greater vibration being generated during machining that damage the machined surface, since the resultant cutting force is almost oriented in the radial direction. From this perspective, stable machining with a tool normal to the surface can rapidly become unstable as the lead angle increases [1]. The surface condition obtained will then very largely depend on the machining strategy chosen [2,3].

Chatter vibration has been well understood since the 1950 s. The first works by Tobias [5] shed light on the mechanism in the case of orthogonal turning. Stability analysis of the machining system then leads to stability mapping being established, in the form of stability lobes. This diagram, representing the limit cutting depth of cut in relation to the spindle speed, enables stable cutting conditions to be chosen (meaning reducing self-excited vibration). This approach was then extended to the case of milling [4]. Consideration for the mean required cutting force, with a linear cutting law, allows analytic or semi-analytic expressions to be obtained, with Budak again promoting such works [6,7].

Furthermore, mathematical methods based on non-linear dynamics allow for extremely fine study of differential equations with delayed terms to model milling, as for example in [8–10]. These approaches that are highly effective in computation time allow for extremely fine modelling of the machining dynamics through consideration for the cutting tool run-out [11], the helix angle [12], use of non-linear cutting laws [13], prediction of Surface Location Error (SLE) [14] and variation in spindle speed [15]. The accuracy of these frequency based methods has again been improved recently [16] and this now makes them highly effective and multi-purpose approaches to the study of stability in machining.

In the case of large chatter amplitude or small radial depth of cut, interrupting cutting in milling introduced a new type of instability, as characterised by one tooth in two actually cutting (flip). This special cutting condition is observable only at high

* Corresponding author. Tel.: +33 5 61 55 77 01; fax: +33 5 61 55 81 78.
E-mail address: landon@cict.fr (Y. Landon).

speed on the first lobes of stability lobes. Flip lobes thus become negligible for high orders [17]. Use of the classical theory developed by Altintas [4] is just as effective, for a negligible calculation time.

In addition to these frequency based approaches, there is another family of approach based on intensive numerical calculation. Here, the cutting forces are calculated and then used in order to simulate the dynamic equation of motion, as with for example [18–22]. Such approaches provide for extremely fine modelling of the dynamics at the scale of chip formation and it is even possible to obtain a 3D representation of the machined surface for systems with extremely simple dynamics [21,23]. Time simulation allows the ploughing effect to be modelled even though this is a rapid phenomenon [24,25] that is highly complex to take into account with frequency based approaches. Recent works modelled the dynamics for 5-axis milling [26] with hemispherical tools for surface machining [27]. This highly comprehensive time-based modelling allows process geometry, cutting force and stability to be obtained. Additional works also present a mathematical model that predicts chatter stability in ball end milling with tool inclination [28].

For the dynamic milling study, a linear cutting law is often used [4,29]. For each angular position of the cutting tool, the cutting force will depend linearly on the cross-section of the chip, i.e.: $Ft = Kt \cdot S$ and $Kr = Fr/Ft$, with Ft the tangential cutting force, Fr the radial cutting force, S the chip cross-section and Kt Kr the specific cutting coefficients. Determining Kt and Kr generally involves an experimental identification, as the accuracy with which they are obtained directly influences the accuracy of the result for maximum allowable axial engagement before the occurrence of regenerative vibrations. The cross-section of the chip must therefore be known exactly. The latter value is determined numerically in order to ensure strong reliability of results. Some works consider a non-linear cutting law for the study of vibrations [30]. However, these authors are confronted by experimental difficulties in correctly measuring the forces in high-speed machining with currently available dynamometers, limited in sampling rate [18].

In the present context, analytical modelling, coupled with a linear cutting law, appears to be the most appropriate approach since it allows for good interaction with the process, rapidity in calculation and the opportunity to perform experimental recalibration [31,32]. With the conventional stability lobes model, optimisation can be applied to the depth of cut and to the spindle speed. Preference is given here to optimisation by spindle speed so as not to bring into question the machining strategy and the CAM process through having to modify the depths of cut.

Many studies have described the stability and the dynamic of the peripheral milling [18–23]. However, few works consider the case of real climb milling, most problematic for mould makers and other manufacturers of complex shaped parts. It therefore remains a challenge to achieve an optimal choice of cutting conditions to improve the quality of cutting locally without degrading the cutter's overall dynamic behaviour.

The aim of this work is to propose a new method to avoid dynamic problem and to increase the metal removal rate for climb milling with a torus mill. The dynamic model is inspired of the classical stability, but new improvements are incorporate. Firstly, an original method is presented to identify the dynamic parameters. Secondly, the start and exit angles are computed exactly using an original numerical model. Thirdly, a sensitivity analysis was conducted in order to study the effect of machining parameters on the stability of climb milling.

The dynamic modelling is presented in section 2. The various specific elements developed to adapt this approach to the case of climb milling are also detailed in this section. An innovative experimental approach, to study stability when climb milling, is described in section 3. Finally, the experimental results are analysed to estimate the accuracy of the model.

2. Dynamic modelling

2.1. Theoretical formulation

The present study is mainly based on Budak's works [6,7], extending them to develop a model. The main assumptions adopted to apply this modelling are as follows:

1. Only the tool is considered to be flexible in so far as the levels of stiffness of the workpiece and the machine tool are so much greater,
2. The tool is modelled by a mass/spring/damper system with 1 degree of freedom along the y direction (cf. Fig. 1),
3. Performance of a linear study allows the static contribution given by feed per tooth to be neglected,
4. The cutting law is linear.

For stability analysis using this model, only the dynamic part of the chip thickness needs to be taken into consideration. This will be a function of the difference between the tooth's position at instant t and the position when the previous tooth strikes at instant $t-\tau$:

$$h(t) = y(t) - y(t-\tau) \tag{1}$$

Using a linear cutting law then allows dynamic cutting forces to be expressed as follows:

$$F_y(t) = \frac{1}{2} \cdot Ap \cdot Kt \cdot [A(t)] \cdot h(t) \tag{2}$$

with Ap the axial depth of cut, Kt the tangential specific cutting coefficient and $[A(t)]$ the matrix of milling dynamic coefficients. In order to reduce computation, only order zero (mean value $[A0]$) of the breakdown into Fourier series decomposition of the matrix $[A(t)]$ is taken into account. The matrix $[A0]$ can then be expressed simply by:

$$[A0] = [\alpha_y] \tag{3}$$

with α_y the milling dynamic coefficient in the y direction. This is expressed by:

$$\alpha_y = \frac{1}{2}[-\cos(2\theta) - 2\theta Kr - Kr\sin(2\theta)]_{\varnothing_s}^{\varnothing_e} \tag{4}$$

with $\varnothing_s$ and $\varnothing_e$ the start and exit angles determined according to the tool's engagement, meaning according to the tilt of the cutting
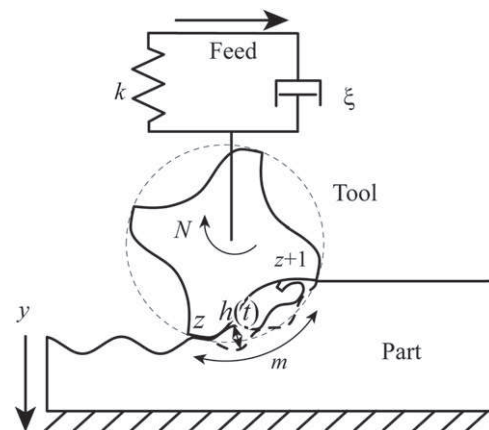

Fig. 1. Tool dynamic modelling.

tool axis in relation to the workpiece, the tool geometry and the depth of cut, and θ the radial engagement angle of the tool, while the reduced radial cutting coefficient is denoted Kr.

The tool is modelled by a system with a single degree of freedom, whose transfer function in the y direction is expressed by the following function:

$$G_y(j\omega_c) = \frac{\omega^2}{k(\omega^2 - \omega_c^2 + j2\xi\omega\omega_c)} \cdot j^2 = -1 \tag{5}$$

with k, ξ and ω respectively the stiffness, the damping ratio and the natural pulsation. Here ω_c corresponds to the chatter frequency. Stability analysis is then conducted by seeking the natural values Λ, a solution to the following characteristic equation:

$$\det([I] + \Lambda[G_y(j\omega_c)]) = 0 \tag{6}$$

In the case of milling, with a system having a single degree of freedom, it is possible to obtain an analytical expression of the limit of stability directly. The limit axial depth of cut before the emergence of chatter is expressed by:

$$A_{plim} = \frac{1}{\frac{z}{2\pi}\alpha_y Kt\,\Re e\left[G_y(j\omega_c)\right]} \tag{7}$$

with z the number of teeth. The real part of the transfer function $G_y(j\omega_c)$ can then be expressed:

$$\Re e[G_y(j\omega_c)] = \frac{1}{k} \times \frac{1-d^2}{(1-d^2)^2 + 4\xi^2 d^2} \text{ avec } d = \frac{\omega_c}{\omega} \tag{8}$$

Finally, the link between the chatter frequency ω_c and the spindle speed N is obtained from the number of entire wavelengths, m, between two teeth passages, that is:

$$N = \frac{60\omega_c}{2z\left[\pi(1+m) - \arctan\left[\frac{d^2-1}{2\xi d}\right]\right]} \tag{9}$$

Then, Eqs. (7) and (9) constitute a system of parametric equations in the form:

$$[Ap(\omega_c); N(\omega_c)]_m \tag{10}$$

with as variable ω_c and m, this last parameter playing a major role as it allows different orders of stability lobes to be dissociated. Finally, a curve is obtained for each value of m, representing a stability lobe.

2.2. Identification

2.2.1. Cutting tool dynamic characteristics

Initially, there is a need to determine the tool dynamic characteristics (stiffness and natural pulsation). The stiffness can be modelled in static, considering the tool to be like a clamped-free beam (cf. Fig. 2).

As the cutting tool geometry is complex, its stiffness cannot be determined by simple calculation of the deformation. An approximate energy method (Ritz method) to calculate the deformation is thus applied. The expression of the tool deformation under a force F applied at the tip is written:

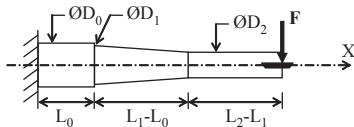$$v(x) = a \cdot x^3 + b \cdot x^2 \tag{11}$$

Fig. 2. Modelling the tool as a clamped-free beam.

The deformation at the tip of the tool $(x = L_2)$ is thus:

$$v(L_2) = a \cdot L_2^3 + b \cdot L_2^2 \tag{12}$$

The moments applied on each portion of the cutting tool are then defined thus:

$$M_0(x) = \frac{\pi \cdot D_0^4}{64} \cdot (v''(x))^2 = \frac{\pi \cdot D_0^4}{64} \cdot (6 \cdot a \cdot x + 2 \cdot b)^2 \cdot x \in [0; L_0] \tag{13}$$

$$M_1(x) = \frac{\pi \cdot \left(D_1 - \frac{D_1 - D_2}{L_1} \cdot x\right)^4}{64} \cdot (6 \cdot a \cdot x + 2 \cdot b)^2 \cdot x \in]L_0; L_1] \tag{14}$$

$$M_2(x) = \frac{\pi \cdot D_2^4}{64} \cdot (6 \cdot a \cdot x + 2 \cdot b)^2 \cdot x \in]L_1; L_2] \tag{15}$$

The energies associated with these moments will then be:

$$W_0 = \frac{E}{2} \cdot \int_0^{L0} M_0(x); W_1 = \frac{E}{2} \cdot \int_{L0}^{L1} M_1(x)p; W_2 = \frac{E}{2} \cdot \int_{L1}^{L2} M_2(x) \tag{16}$$

With E Young's modulus.

The total potential energy can then be expressed:

$$EPT(a,b) = W_0 + W_1 + W_2 - F \cdot v(L_2) = W_0 + W_1 + W_2 - F \cdot \left(a \cdot L_2^3 + b \cdot L_2^2\right) \tag{17}$$

Coefficients a and b are then determined by minimising the total potential energy:

$$\frac{\partial EPT(a,b)}{\partial a} = 0 \text{ and } \frac{\partial EPT(a,b)}{\partial b} = 0 \tag{18}$$

The values for a and b can then be reinjected into Eq. (12) in order to calculate the deformation at the tip of the tool. The stiffness is thus obtained:

$$k = \frac{F}{v(L_2)} \tag{19}$$

Numerical application is performed in the case of the cutting tool used in this article. As diameters D_0, D_1 and D_2 have respective values 10 mm, 9 mm and 7.5 mm, lengths L_0, L_1 and L_2 come respectively to 0 mm, 20 mm and 39 mm and with the Young's modulus taken equal to 210 GPa, static stiffness of the tool k of 2473 N/mm is obtained.

Moreover, the natural frequency for this cutting tool can be determined by the Rayleigh method, approximating the tool by a cylinder with diameter D_{eq} and density $\rho = 7.800$ kg/m³:

$$f_n = \frac{\omega_n}{2 \cdot \pi} \text{ with } \omega_n^2 = 12.36 \cdot E \cdot \frac{\pi \cdot D_{eq}^4}{64} \cdot \frac{1}{\rho \cdot S \cdot L_2^4} \text{ where } S = \frac{\pi \cdot D_{eq}^2}{4} \tag{20}$$

The equivalent diameter of the tool is determined from the stiffness value obtained previously. A cylindrical milling cutting tool with length L_2, stiffness k and Young's modulus 210 GPa has for diameter 8.299 mm. D_{eq} is thus taken to be equal to that value. The natural frequency for the tool is then evaluated at 3960 Hz.

These parameters were also determined experimentally using a laser vibrometer. The static stiffness measured was 2720 N/mm, that is a deviation of 9% as compared with the value obtained by computation. The natural frequency measured meanwhile was 4040 Hz, which is a deviation by 1.9% as compared with the calculated value. This validates the method used in calculating the tool dynamic characteristics.

2.2.2. Chip cross-sections

Experimental identification of the cutting coefficients Kt and Kr requires precise knowledge of how the chip cross-section evolves throughout a tooth's cutting phase. In the case of milling with lead angle using a torus mill, in order to determine the chip

cross-section at a given instant, two toroids T_1 and T_2 represent the envelope of the cutting part of the tool on passing of two successive teeth. Obviously, this representation is a simplification as compared with the real envelope of the cutting part of the tool, as the centre of the insert describes a cycloid. But this simplification has no incidence on the validity of the calculation given that the tool radius considered is large as compared with feed per tooth ($fz=0.05$ to 0.15 mm/tooth) [33,34].

The toroids T_1 and T_2 can be represented by parameterised surfaces $T_1(u_1,v_1)$ and $T_2(u_2,v_2)$. To compute the chip cross-section, the distance between surfaces $T_1(u_1,v_1)$ and $T_2(u_2,v_2)$ is considered. For each point (u_1,v_1) of T_1, this distance is calculated by positing:

$$T_1(u_1,v_1)+d.n(u_1,v_1)=T_2(u_2,v_2) \tag{21}$$

where $n(u_1,v_1)$ is the normal to $T_1(u_1,v_1)$ at point (u_1,v_1).

Eq. (21) is a system of 3 equations with 3 unknowns (d, u_2 and v_2) that can be resolved extremely rapidly using the Newton–Raphson method. The value d thus obtained expresses the distance between the two toroids (Fig. 3).

By scanning the parametric domain, the chip thickness can thus be calculated at a given point from entry of the insert into the material through to its exit. By scanning the parametric domain on v for a given value u, a set of values d_i is obtained corresponding to a same chip cross-section (Fig. 4). The surface S_c of this cross-section can then be calculated by:

$$S_c = \sum_i \left[\frac{(r+d_{i+1})^2 + (r+d_i)^2}{4} \cdot dv - \frac{r^2}{2} \cdot dv \right] \tag{22}$$

From the chip cross-sections thus calculated, the cutting force coefficients Kt and Kr can then be identified during instrumented tests. This requires precise calculation of the start and exit angles of the tooth in the material.

2.2.3. Start and exit angles

Application of the stability lobes theory requires calculation of start and exit angles Øs and Øe of a tool tooth in the material (Fig. 5).

These angles are difficult to determine analytically in the most general case. It is preferable to determine them numerically during the procedure used to calculate the chip cross-section. Indeed, when the distance between the two toroids is negative or null, this means that there is an intersection between passage of a tooth and passage of the next tooth. The max. and min. values of u for which the chip thickness is null thus provide angles $Ø_s$ and $Ø_e$ directly.
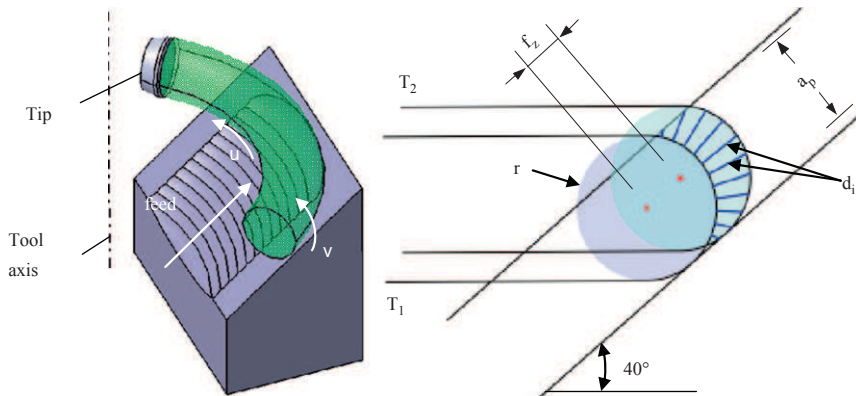
2.2.4. Determining mean values for Kt and Kr

From calculation of the start and exit angles for the insert in the material, it is possible to extract the forces measured over that angular range for each test performed so as to identify coefficients Kt and Kr experimentally. The difficulty lies in extracting a unique couple of coefficients (Kt,Kr), as needed for stability theory, from many values derived from the measurements.

To do so, the cutting forces are measured for several couples of axial engagement—feed per tooth cutting conditions. The cutting force measurement was performed using a three component Kistler 9257BA dynamometer.

For each of the measurements made, the tangential and radial forces are determined. Then, for each measurement increment, the tangential force is divided by the cross-section of the chip corresponding to the associated angular position. This gives a value of Kt_{θ} for each angular position θ of the tool. Similarly, a coefficient Kr_{θ} is extracted from the ratio between the radial force and the tangential force. Thus, for each measurement the evolution of coefficients Kt and Kr in relation to the angular position for the tooth considered is obtained.

Next, these coefficients are averaged over the cutting angular range, then over all the tool rotations measured.

Six tests were conducted under different cutting conditions so as to quantify the variation in coefficients Kt and Kr in relation to the said conditions. Thus, seven couples of coefficients (Kt, Kr) were obtained (Fig. 6).

Variation in the coefficients over the set of tests remains acceptable and allows a unique couple of coefficients that can be used in the stability theory to be extracted. The final values for coefficients Kt_M and Kr_M are then obtained by averaging the values calculated for each test. The following is then obtained:

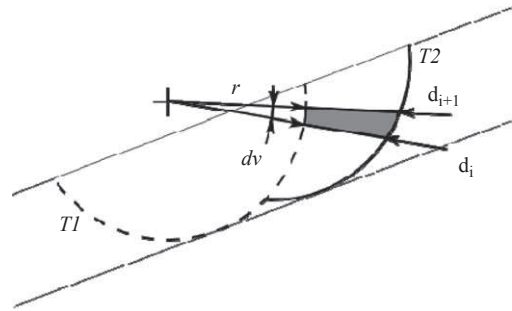$$Kt_M = 2935 \text{ N/mm}^2 \pm 12\%$$

$$Kr_M = 0.343 \pm 8\%$$

Fig. 4. Calculating instantaneous chip cross-sections.

Fig. 3. Calculating the chip cross-section.

2.3. Plotting the stability lobes

Plotting the stability lobes is conducted in accordance with the classical theory developed by Altintas as recalled in section 2.1. In the case of a low radial engagement, the conventional model does not integrate cutting discontinuities. In order to check this model's validity, the lobes were also plotted using the Semi-Discretisation Method (SDM) developed by Insperger [16]. This approach takes into account cutting discontinuity. The tool's modal characteristics together with machining characteristics are summarised in Table 1. The curve of stability lobes with the two approaches is shown in Fig. 7. Slight differences appear between the two plots. These are easily explained since, with SDM, extremely fine discretisation is needed to be able to observe lobes of high orders (here the 14th). However, in the present context, the cutting discontinuity does not modify the optimum spindle speeds (low influence of cutting discontinuity), as both curves show the same optimum regions. Furthermore, the conventional approach is more safety oriented. Thus, the order of the lobes is high (14th) and the influence of the flip lobes can be neglected. The remainder of the present study will therefore use the classical theory developed by Altintas; the corresponding curve for stability lobes is shown in Fig. 8.

2.4. Uncertainties as to stability lobe curves

It was shown that identification of the coefficients Kt and Kr leads to determination of a couple of values with uncertainty for each of them related to the variation in the values obtained for the different measurements made.

The same applies for the other parameters in stability lobes theory. Thus, in order to identify critical parameters in relation to the accuracy of stability lobe plot, a study of the influence of either parameter was conducted. To do so, a variation by $\pm 10\%$ was associated with each parameter (stiffness k, damping ξ, coefficients Kt and Kr, and the $\emptyset s$ and $\emptyset e$ start and exit angles). The results of sensibility are shown in Figs. 9 and 10.

As the region of interest for stability is located under the intersection of two consecutive lobes, at around 16,000 rpm (Figs. 9 and 10), several conclusions can be deduced from this observation.

Firstly, it appears that a variation in the value of damping has a non-significant influence in this region (Fig. 9b). The study of the influence of a greater variation in this parameter validated this conclusion. Thus, it is not essential to refine determination of the damping parameter as long as work continues to be pursued in the region of interest for stability.

Next, the influence of parameters k, Kt and Kr are identical (Figs. 9a and c). A variation by $\pm 10\%$ in their respective values generates uncertainty of the same order of magnitude ($\pm 10\%$) on the stability lobes curve in the region of interest (evaluated at the

Table 1
Parameters used to plot stability lobes.

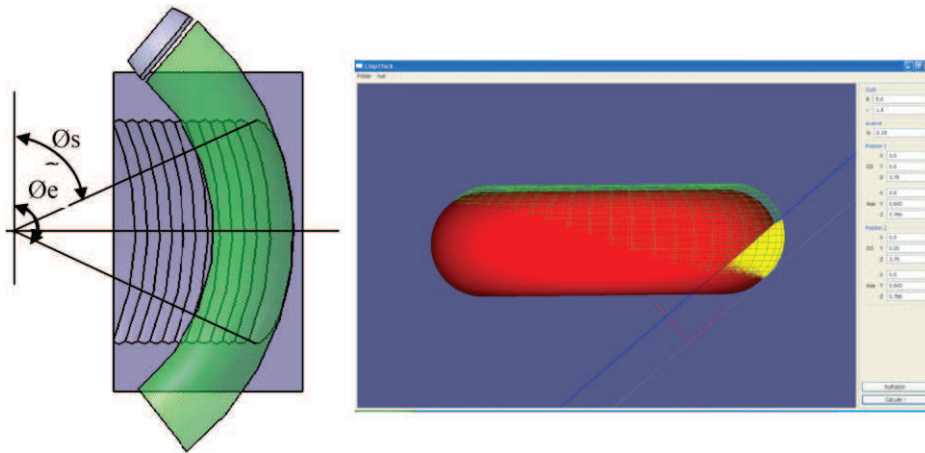| Characteristic	Value
Natural frequency	4,040 Hz
Modal stiffness	2720 N/mm
Damping ratio	0.45%
Tool number of teeth	1
Tool radius	4 mm
Radial depth of cut	0.1 mm
Tangential cutting coefficient Kt	2935 MPa
Reduced cutting coefficient Kr	0.343

Fig. 5. Calculating start and exit angles in the material and picture of the numerical model.
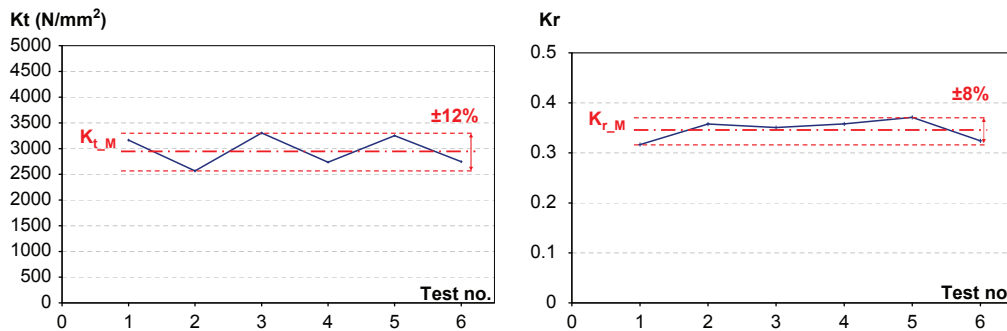

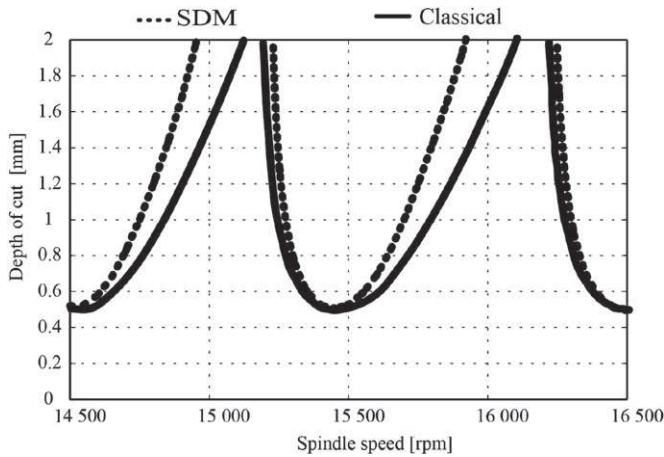**Fig. 6.** Evolution of cutting force coefficients Kt and Kr over the entire set of tests.

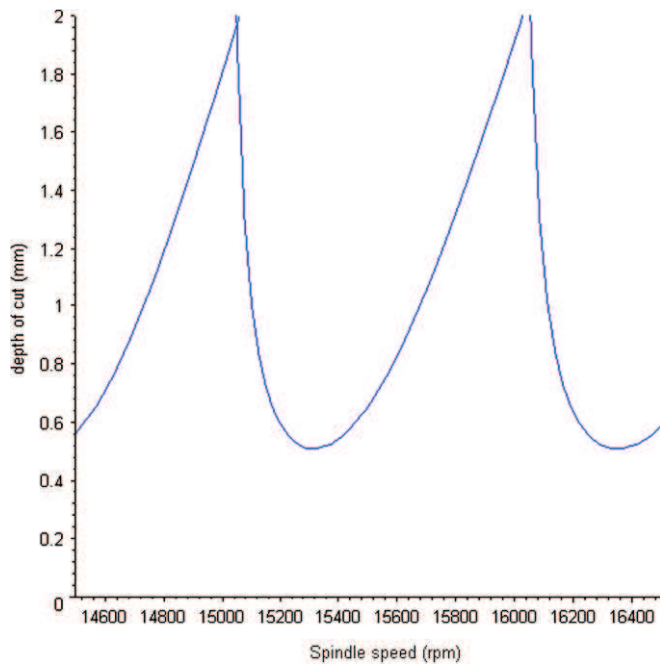**Fig. 7.** Comparison of stability lobe curves.

Fig. 8. Stability lobes for torus tool at around 15,000 rpm.

position of the intersection point between two consecutive lobes). These three parameters therefore need to be determined as finely as possible. The method proposed here seeks to identify these values accurately.

Finally, the influence of a variation by $\pm 10\%$ in the start and exit values generates major uncertainty (-20.31%; $+29.17\%$, evaluated at the position of the point of intersection between two consecutive lobes) in the curve of the lobes (Fig. 10). This parameter is thus the critical parameter with respect to uncertainty on the stability lobes curve. This justifies the necessity of precise determination of the start and exit angles, by a specific numerical method. Thus, the effective variation of these angles is essentially due to vibrations during machining.

Similarly, a variation by $\pm 10\%$ of the natural frequency was simulated (Fig. 11).

This variation's influence significantly affects the horizontal position of the stability lobes. Here again, this justifies implementation in the present methodology of a model for estimation of the natural frequency related to a precise experimental

identification. The uncertainty obtained is of just 1.9%, thus limiting uncertainty on the stability lobes curve.

3. Experimental study

3.1. Experimental setup

The modelling proposed was confronted with an experimental study. Milling tests with different lead angle values (between 10 and 60° by 10° increments) were conducted to this purpose. The results presented in the present article concern the case of a 40° lead angle. The cutting tool used was a Ø8 mm P15 uncoated carbide mill with Ø5 mm round insert (as modelled in section 2.2.1). The tool was chuck collet mounted with a free length of 39 mm, the value used in modelling. The tests were conducted on solid C40 steel workpieces. The machine used was DMG DMU 50 eVo 5-axis machining centre equipped with a Siemens 840D control system. The experimental setup is shown in Fig. 12.

In order to validate the presence of chatter vibrations and determine the vibrations frequencies, two types of vibration measurements were made. The first involved acoustic acquisition of the machining operation. The advantage of this type of measurement lies in it being easy to set up in a production workshop. In parallel, a laser velocimeter was used to identify the vibration frequencies and modal damping. It is also useful in validating the use of acoustic measurements for frequency identification of regenerative vibrations in machining.

For acoustic acquisition, the following equipment (Fig. 13) was used:

1. 1 hypercardioid directivity broad membrane static microphone placed outside the work chamber due to its considerable fragility.
2. 1 cardioid directivity SM58 Shure dynamic microphone placed inside the chamber above the machining zone.
3. a preamplifier/limiter placed upstream of the digitising system comprising a USB2 TASCAM US428 interface and a PC equipped with a dedicated audio acquisition software package.

The tool vibrations were measured using a laser velocimeter (Ometron, VH300+). This instrument is capable of measuring the vibration of a rotating tool and the laser beam is simply focused on a cylindrical part of the tool. The spot size of the laser is adjusted to approximately 1 mm in order to average the scale of the surface roughness. The laser beam is easy to use in an industrial environment since it is contact-free.

Finally, some tests were filmed using a high-speed camera. The camera used was an X-STREAM VISION controlled by the X-Vision software. Using an adjustable objective, the camera was placed at a distance of 1.5 m from the plate so as to be free of disturbance from the machine. A 1000 W projector was used to illuminate the drilling observation area. An acquisition frequency of 30,000 images per second was used. The videos obtained allowed the tool's dynamic behaviour and the cutting vibration sequence to be observed. The results are given below. This type of observation of tool dynamic behaviour during climb milling is original and constitutes an innovative and effective mean to observe and better understand the rapid phenomena that come into play in machining.

3.2. Experimental strategy

As the main objective was to validate modelling implemented on the basis of stability lobes, various types of tests were performed. The tests involved frequency scanning at a given
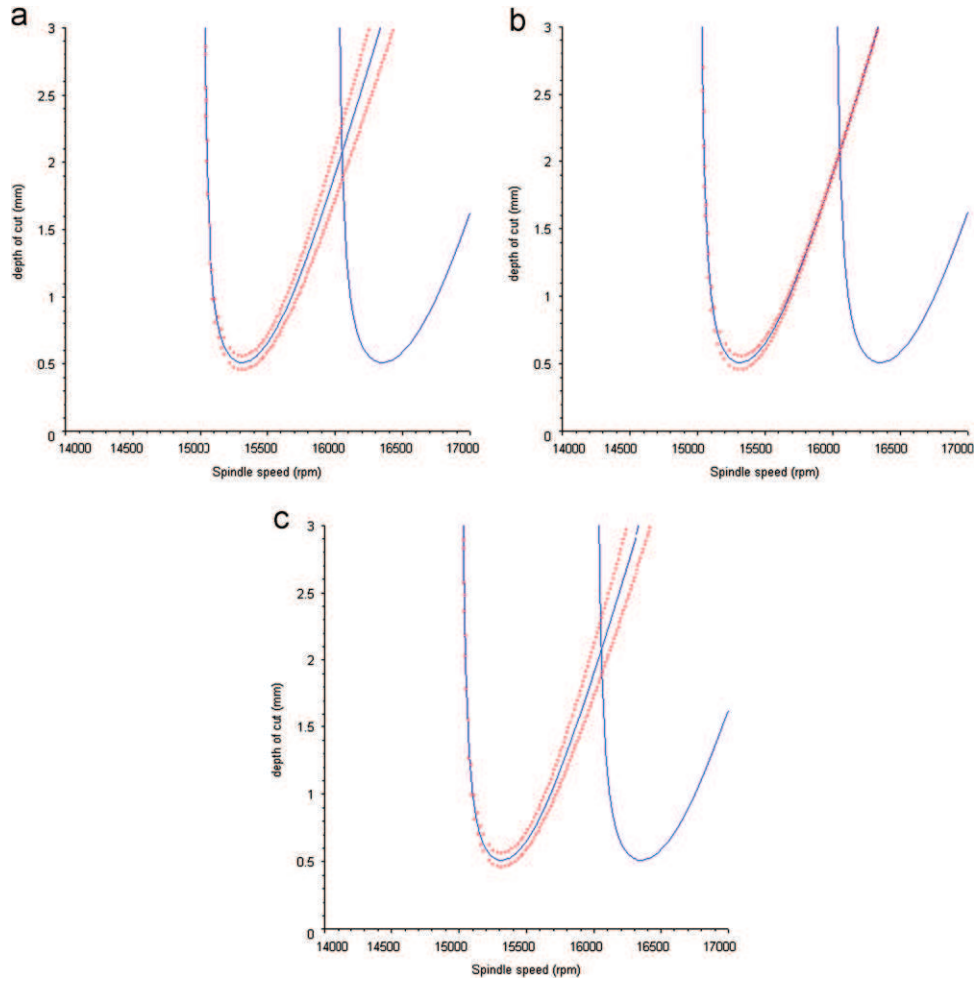
Fig. 9. Influence of a variation by $\pm$ 10% in stiffness k (a), damping ξ (b) and coefficient Kt or Kr (c) on the curve of a lobe.
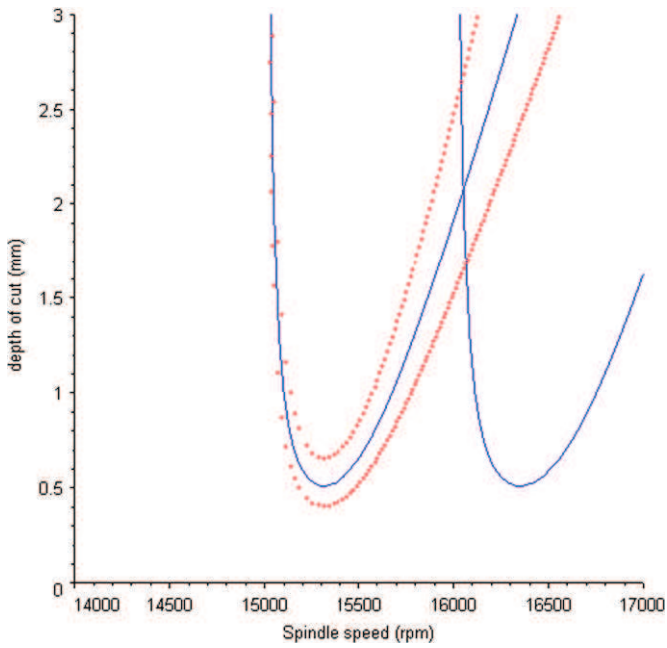

Fig. 10. Influence of a variation by $\pm$ 10% of the Ø start angle on the curve of a lobe.
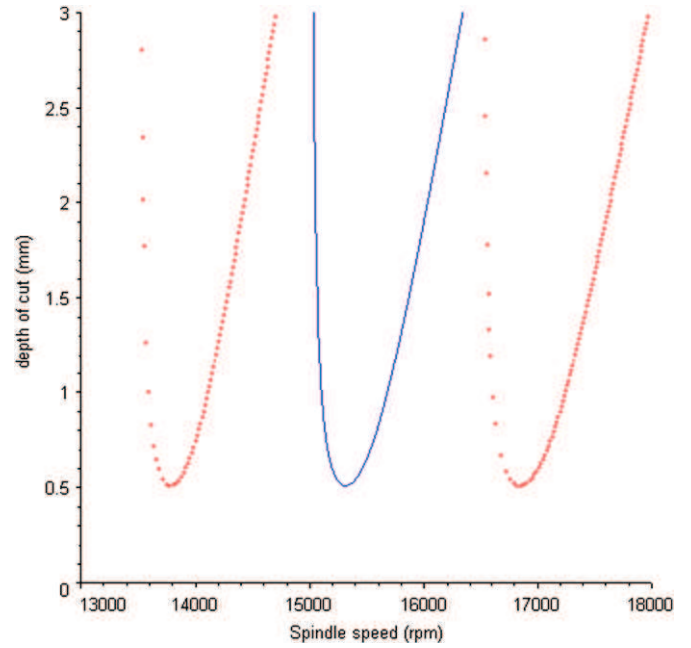
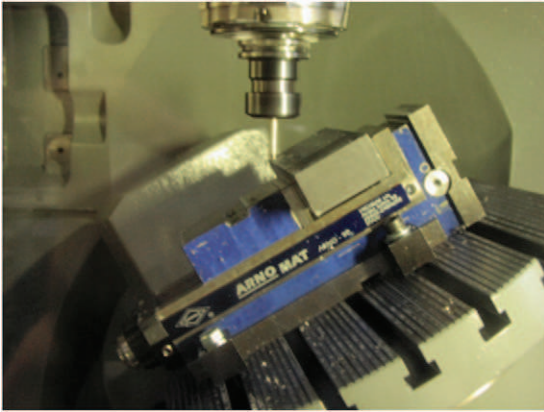**Fig. 11.** Influence of a variation by $\pm$ 10% of the natural frequency fn on the curve of a lobe.
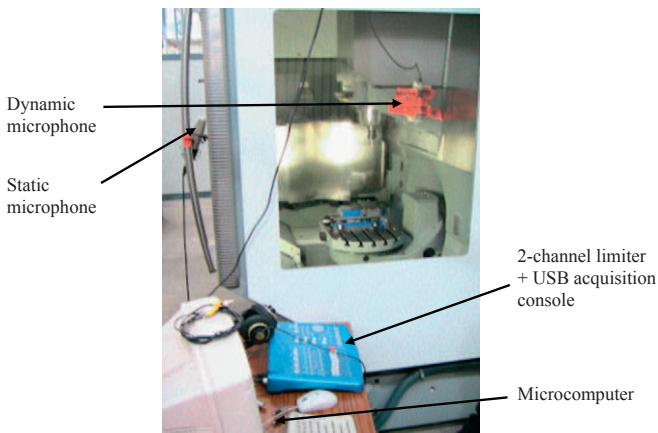
Fig. 12. Experimental setup.

Dynamic microphone

Static microphone

2-channel limiter + USB acquisition console

Microcomputer

Fig. 13. Acoustic measurement system.

Frequency scanning

Cutting depth scanning

Fig. 14. Frequency and cutting depth scanning strategy.

≈ Unstable machining

= Stable machining

Fig. 15. Correlation between modelling and experimental observations at around 5000 rpm.

cutting depth and scanning in engagement at a given spindle speed (Fig. 14).

For the frequency scanning tests, two central spindle speeds were chosen. The first corresponded to the tool manufacturer's cutting recommendations, i.e. 5000 rpm. The second, at 15,000 rpm, was chosen well above this value so as to validate dynamic modelling at high speed. A scan around these central values was made per 10 rpm increment in the first case and by 100 rpm in the second case. The aim was to observe successive stable/unstable states on frequency scanning in order to validate the horizontal position of the lobes derived from modelling (uncertainty on natural frequency fn). The depth of cut retained for these tests was 0.75 mm and 1 mm, these values being chosen from modelling to observe successive stable and unstable states.

These first tests allowed spindle speeds leading to machining that could be qualified as stable (15,000 rpm) or unstable (5050 rpm and 15,300 rpm) to be identified. For these three noteworthy spindle speeds, a cutting depth scan was made while varying the axial engagement between 0.4 and 2 mm so as to identify the limit axial engagement ap_{lim} for each frequency.

4. Analysis of results

Analysis of the results involved confronting the experimental results with the model. To do so, it had to be determined for each test whether the cutting phenomenon was stable or unstable (presence of regenerative vibrations). Acoustic and laser velocimeter measurements made were analysed to this purpose. After FFT processing of the acquisitions, the presence of regenerative
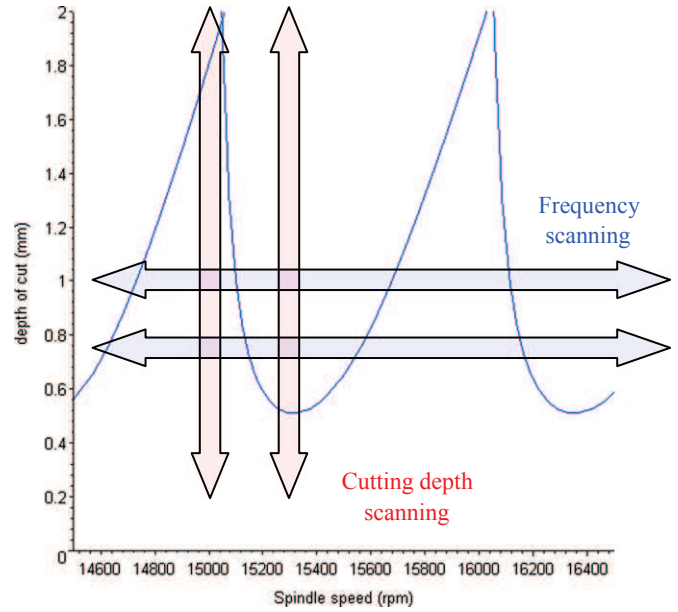
vibrations was expressed by the appearance of a high-amplitude, high-frequency peak close to the natural frequency of the tool (determined at 4,040 Hz). This peak was absent when machining was stable. A distinction could thus be made between stable and unstable tests.

4.1. Tests at different spindle speeds

Frequency scanning was initially performed for spindle speeds of between 5,000 and 5100 rpm with 10 rpm increments. The results obtained are shown in Fig. 15. The symbol ≈ represents a test showing instability (presence of regenerative vibrations). The symbol = represents a test during which cutting was stable (absence of regenerative vibrations). The tests performed around 5000 rpm with a cutting depth of 1 mm all showed pronounced instability. With a

cutting depth of 0.75 mm, cutting remained stable for tests at 5,010 and 5,020 rpm. This concurs with the theoretical modelling adopted.

Frequency scanning was also performed for spindle speeds of between 14,600 and 16,300 rpm with 100 rpm increments and for a cutting depth of 1 mm. The results obtained are shown in Fig. 16. It appears experimentally that the tests performed between 14,800 and 15,100 rpm, then between 15,700 and 16,100 rpm show stable cutting, free from regenerative vibrations. Outside these intervals, cutting was unstable and the surface condition strongly degraded. Here too, the experimental observations backed up the theoretical model developed.

Over all the tests under unstable cutting conditions, surface condition measurements performed using a 3D optical roughness metre (WYKO NT 1,100 optical profiler) showed a mean roughness of Rt 69.62 μm in the direction of feed (Fig. 16). For the stable tests, a mean Rt of around 0.82 μm was generally observed. These readings show the direct impact the presence of regenerative vibrations has on the surface roughness. The pictures captured using a high-speed camera also showed the presence of instability and permitted to validate assumptions made relating to cutting continuity and allowing a classical approach for stability study to be applied (the video can be watched at http://www.youtube.com/watch?v=voU6bDKi2JE).

After this first frequency scanning test campaign, the proposed modelling very effectively predicts the spindle speed intervals to ensure stable cutting. The following tests are intended to validate the vertical position of the curve.

4.2. Tests at different depths of cut

With the aim of identifying the limit axial depth of cut and validating the vertical position of the theoretical stability lobes, cutting depth scanning was performed. The axial depth of cut varies between 0.5 and 2 mm for spindle speeds previously identified as leading to stable (5,010 rpm for $ap = 0.75$ mm and 15,000 rpm for $ap = 1$ mm) or unstable (5,050 and 15,300 rpm for $ap = 1$ mm) cutting. These tests led to the results shown in Fig. 17.

Overall, considering the comparisons made, the very good correlation between the forecast and the experimental results means that the proposed approach and modelling can be validated. However, some tests that were predicted as being stable from the modelling, though close to the stability limit, appear to be experimentally unstable. The vertical position of the stability lobes obtained by the modelling proposed is thus slightly over-estimated (error of the order of 5%). This confirms the study conducted previously on modelling uncertainty. Indeed, it has been shown that uncertainty in determining certain parameters results in inaccuracy on the vertical position of the stability lobes. This justifies the modelling recommended, as based on that uncertainty being taken into account. More precise determination of the limit axial depth of cut will require the pursuit of an experimental campaign in order to recalibrate the model.

5. Conclusions

In this article, stability and dynamic behaviour of climb milling was investigated for a torus mill on 5 positioned axes. Based on both the simulation and experimental investigation, the following points are made clear:

(1) The classical stability lobes theory is readily applicable to predict the dynamic behaviour of a torus mill in climb milling. In the present study, this extremely simple approach, as widely used industrially, shows the same optimum regions as the more sophisticated method of semi-discretisation. For high orders, the flip lobe and thus cutting discontinuity can readily be neglected. The use of high-speed cameras in a context of torus mill vibration represents a rapid and innovative way to better understand and model dynamic behaviour. Assumptions relating to cutting continuity were thus validated, allowing a classical approach for stability study to be applied.

(2) The sensitivity analysis shows that the uncertainty due to dynamic parameters identification has a direct influence on
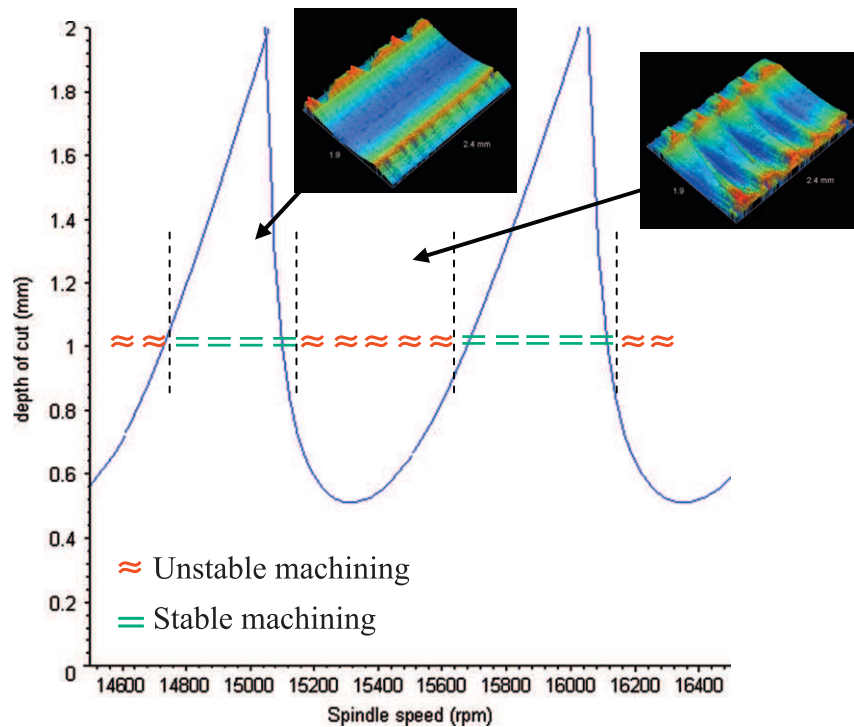

Fig. 16. Correlation between modelling at around 15,000 rpm and experimental observations.
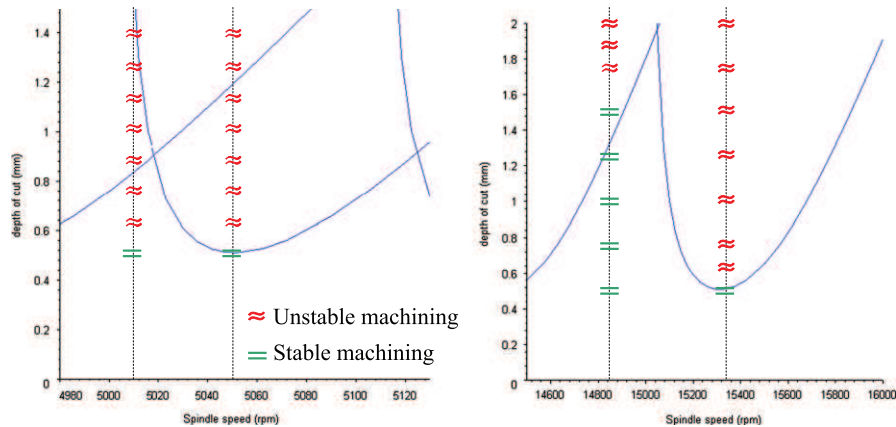
Fig. 17. Correlation between stability lobes and experimental observations around 5000 rpm and 15,000 rpm.

stability limit accuracy. Tool dynamic characteristics, start and exit angles, as cutting coefficients (Kt,Kr), must be precisely identified. Tool dynamic characteristics (stiffness and natural pulsation) can be more precisely determined by using a new coupled calculations-tests method. Start and exit angles can be computed exactly using a numerical model of the milling configuration.

(3) It was shown that a third region of "potential instability" needed to be taken into account in plotting stability lobes due to the uncertainty of prediction due to modelling and identification of parameters.

(4) The approach proposed involving identification of the parameters for the model is validated by a confrontation of the prediction with experimental results.

(5) This work makes it possible to provide a tool to support the CAM process, allowing the operator to choose, or limit, the lead angle according to the tool used.

(6) The proposed approach paves the way for 3D stability mapping representing the influence of the tool/surface inclination in the third dimension.

Acknowledgements

References

[1] E. Ozturk, L.T. Tunc, E. Budak, Investigation of lead and tilt angle effects in 5-axis ball-end milling processes, International Journal of Machine Tools and Manufacture 49 (2009) 1053–1062.

[2] Y. Quinsat, S. Lavernhe, C. Lartigue, Characterization of 3D surface topography in 5-axis milling, Wear 271 (2011) 590–595.

[3] X. Pessoles, Y. Landon, W. Rubio, Kinematic modelling of a 3-axis NC machine tool in linear and circular interpolation, International Journal of Advanced Manufacturing Technology 47 (2010) 639–655.

[4] Y. Altintas, E. Budak, Analytical prediction of stability lobes in milling, Annals of the CIRP 44 (1995) 357–362.

[5] S.A. Tobias, W. Fishwick, Theory of regenerative machine tool chatter, Engineer 205 (199–203) (1958) 238–239.

[6] E. Budak, Analytical models for high performance milling—Part I: cutting forces, structural deformations and tolerance integrity, International Journal of Machine Tools and Manufacture 46 (2006) 1478–1488.

[7] E. Budak, Analytical models for high performance milling—Part II: process dynamics and stability, International Journal of Machine Tools and Manufacture 46 (2006) 1489–1499.

[8] M.A. Davies, J.R. Pratt, B. Dutterer, T.J. Burns, Stability prediction for low radial immersion milling, Transactions of the ASME, Journal of Manufacturing Science and Engineering 124 (2002) 217–225.

[9] P.V. Bayly, J.E. Halley, B.P. Mann, M.A. Davies, Stability of interrupted cutting by temporal finite element analysis, Transactions of the ASME, Journal of Manufacturing Science and Engineering 125 (2003) 220–225.

[10] T. Insperger, G. Stepan, Updated semi-discretization method for periodic delay-differential equations with discrete delay, International Journal for Numerical Methods in Engineering 61 (2004) 117–141.

[11] T. Insperger, B.P. Mann, T. Surmann, G. Stepan, On the chatter frequencies of milling processes with runout, International Journal of Machine Tools and Manufacture 48 (2008) 1081–1089.

[12] M. Zatarain, J. Munoa, G. Peigne, T. Insperger, Analysis of the influence of mill helix angle on chatter stability, Annals of the CIRP 55 (2006) 365–368.

[13] G. Stepan, R. Szalai, B.P. Mann, P.V. Bayly, T. Insperger, J. Gradisek, E. GOVEKAR, Nonlinear dynamics of high-speed milling—analyses, numerics, and experiments, Transactions of the ASME, Journal of Vibration and Acoustics 127 (2005) 197–203.

[14] T. Insperger, J. Gradisek, M. Kalveram, G. Stepan, K. Weinert, E. Govekar, Machine tool chatter and surface location error in milling processes, transactions of the ASME, Journal of Manufacturing Science and Engineering 128 (2006) 913–920.

[15] S. Seguy, T. Insperger, L. Arnaud, G. Dessein, G. Peigne, Suppression of period doubling chatter in high-speed milling by spindle speed variation, Machining Science and Technology 15 (2011) 153–171.

[16] T. Insperger, G. Stepan, J. Turi, On the higher-order semi-discretizations for periodic delayed systems, Journal of Sound and Vibration 313 (2008) 334–341.

[17] J. Gradisek, M. Kalveram, T. Insperger, K. Weinert, G. Stepan, E. Govekar, I. Grabec, On stability prediction for milling, International Journal of Machine Tools and Manufacture 45 (2005) 769–781.

[18] F. Lapujoulade, T. Mabrouki, K. Raissi, Prédiction du comportement vibratoire du fraisage latéral de finition des pièces à parois minces, Mécanique et Industries 3 (2002) 403–418.

[19] M.L. Campomanes, Y. Altintas, An improved time domain simulation for dynamic milling at small radial immersions, Transactions of the ASME, Journal of Manufacturing Science and Engineering 125 (2003) 416–422.

[20] X. Liu, K. Cheng, Modelling the machining of peripheral milling, International Journal of Machine Tools and Manufacture 45 (2005) 1301–1320.

[21] T. Surmann, D. Enk, Simulation of milling tool vibration trajectories along changing engagement conditions, International Journal of Machine Tools and Manufacture 47 (2007) 1442–1448.

[22] L. Arnaud, O. Gonzalo, S. Seguy, H. Jauregi, G. Peigne, Simulation of low rigidity part machining applied to thin walled structures, International Journal of Advanced Manufacturing Technology 54 (2011) 479–488.

[23] P. Lorong, G. Coffignal, E. Balmes, M. Guskov, A. Texier, Simulation of a finishing operation: milling of a turbine blade and influence of damping, in: Proceedings of ASME 2012 11th Biennal Conference on Engineering Systems design and analysis, ESDA 2012, July 2–4, 2012, Nantes, France.

[24] S. Seguy, G. Dessein, L. Arnaud, Surface roughness variation of thin wall milling, related to modal interactions, International Journal of Machine Tools and Manufacture 48 (2008) 261–274.

[25] K. Ahmadi, F. Ismail, Analytical stability lobes including nonlinear process damping effect on machining chatter, International Journal of Machine Tools and Manufacture 51 (2011) 296–308.

[26] K. Ahmadi, F. Ismail, Machining chatter in flank milling, International Journal of Machine Tools and Manufacture 51 (2010) 75–85.

[27] E. Budak, E. Ozturk, L.T. Tunc, Modelling and simulation of 5-axis milling processes, Annals of the CIRP 58 (2009) 347–350.

[28] E. Shamoto, K. Akazawa, Analytical prediction of chatter stability in ball end milling with tool inclination, Annals of the CIR 58 (2009) 351–354.

[29] S. Engin, Y. Altintas, Mechanics and dynamics of general milling cutters, part II: inserted cutters, International Journal of Machine Tools and Manufacture 41 (2001) 2213–2231.

[30] H. Paris, D. Brissaud, A. Gouskov, A more realistic cutting force model at uncut chip thickness close to zero, Annals of the CIRP 56 (2007) 415–418.

[31] V. Thevenot, L. Arnaud, G. Dessein, G. Cazenave-Larroche, Integration of dynamic behaviour in stability lobes method: 3D lobes construction and application to thin walled structure milling, International Journal of Advanced Manufacturing Technology 27 (2006) 638–644.

[32] S. Seguy, F.J. Campa, L.N. Lopez De Lacalle, L. Arnaud, G. Dessein, G. Aramendi, Toolpath dependent stability lobes for the milling of thin-walled parts, International Journal of Machining and Machinability of Materials 4 (2008) 377–392.

[33] Y. Landon, S. Segonds, M. Mousseigne, P. Lagarrigue, Correction of milling tool paths by Tool Positioning Defect (TPD) compensation, Institution of Mechanical Engineers (I MECH E) Part B—Journal of Engineering Manufacture 217 (2003) 1063–1073.

[34] S. Segonds, Y. Landon, F. Monies, P. Lagarrigue, Method for rapid characterisation of cutting forces in end milling considering runout, International Journal of Machining and Machinability of Materials 1 (2006) 45–61.